

Sediment biomarkers record hydrological and anthropogenic-driven environmental changes since 1800 AD in the Ili-Balkhash Basin, arid Central Asia

Hongliang Zhang,^{1,2} Jinglu Wu,^{1,2,3*} Long Ma,³ Shuie Zhan,^{1,2} Miao Jin,^{1,2} Zhangdong Jin⁴

¹State Key Laboratory of Lake Science and Environment, Nanjing Institute of Geography and Limnology, Chinese Academy of Sciences, Nanjing; ²University of Chinese Academy of Sciences, Beijing; ³Research Center for Ecology and Environment of Central Asia, Chinese Academy of Sciences, Urumqi; ⁴State Key Laboratory of Loess and Quaternary Geology, Institute of Earth Environment, Chinese Academy of Sciences, Xi'an, China

ABSTRACT

Human activity and hydroclimate change greatly influence the environment in a lake and its catchment, particularly in areas with fragile ecosystems, such as arid Central Asia. In this study, lipid biomarkers (*n*-alkanes and *n*-fatty acids) were measured in a ²¹⁰Pb- and ¹³⁷Cs-dated sediment core from Lake Balkhash to determine their environmental significance and infer the history of environmental change over the last ~200 years. The terrestrial origin of long-chain *n*-alkanes and the aquatic origin of both *n*-fatty acids and mid-/short-chain *n*-alkanes were inferred from molecular distributions and diagnostic ratios. Three major environmental phases were identified over the past two centuries based on stratigraphic shifts in biomarker indicators. During 1800-1860 AD, the lake exhibited a high-water level with abundant submerged/floating macrophytes and limited phytoplankton, as suggested by multiple indicators, *e.g.*, high proportions of aquatic macrophytes (Paq) and long-chain *n*-fatty acids (L-FAs). Overall, minor terrestrial inputs were revealed by low concentrations of long-chain *n*-alkanes (L-ALKs), suggesting dense vegetation cover in the catchment. The lake environment experienced a pronounced change in the subsequent phase from 1860-1930 AD, during which the cover of submerged/floating macrophytes gradually diminished, as revealed by the decreasing trend of aquatic proxies, *e.g.*, L-FAs and Paq. In contrast, the number of emergent plants and terrestrial inputs increased, as suggested by the decreased Paq values. A great variation in water levels likely resulted in the shrinkage of the submerged/floating macrophyte cover. During 1930-2017 AD, anthropogenic impacts began to appear on the sediment profile. The highest terrestrial inputs, as revealed by the maximum L-ALK abundance on record, indicated intensive exploitation of the catchment during 1935-1959 AD. The lowest L-FA and Paq values suggested that submerged/floating macrophytes were at the lowest levels during

this phase, possibly in response to the decreased water levels and increasing salinity. Increased human-induced nutrient loading coupled with elevated regional temperature prompted the lake to become an increasingly productive lake system, especially in more recent decades, as indicated by the highest levels of short-chain lipids. These results highlight the important role of hydrological variation and human activity in the environmental evolution of the Ili-Balkhash Basin.

*Corresponding author: w.jinglu@niglas.ac.cn

Key words: lipid biomarker; environmental evolution; hydrological change; anthropogenic impact; Ili-Balkhash Basin.

Citation: Zhang H, Wu J, Ma L, Zhan S, Jin M, Jin Z. Sediment biomarkers record hydrological and anthropogenic-driven environmental changes since 1800 AD in the Ili-Balkhash Basin, arid Central Asia. *J Limnol* 2024;83:2106.

Edited by: Andrea Lami, *National Research Council, Water Research Institute (CNR-IRSA), Verbania Pallanza, Italy.*

Received: 22 November 2022.

Accepted: 8 February 2024.

Publisher's note: all claims expressed in this article are solely those of the authors and do not necessarily represent those of their affiliated organizations, or those of the publisher, the editors and the reviewers. Any product that may be evaluated in this article or claim that may be made by its manufacturer is not guaranteed or endorsed by the publisher.

©Copyright: the Author(s), 2024

Licensee PAGEPress, Italy

J. Limnol., 2024; 83:2106

DOI: 10.4081/jlimnol.2024.2106

This work is licensed under a Creative Commons Attribution-NonCommercial 4.0 International License (CC BY-NC 4.0).

INTRODUCTION

Arid Central Asia (ACA) is one of the most environmentally sensitive areas on Earth, and lakes in ACA are especially important for this fragile environment and for ensuring the livelihoods of local residents (Mischke, 2020). Lake Balkhash is now the largest lake in ACA after the desiccation of the Aral Sea and is critical for the region not only because of its economic contributions, such as local fisheries and irrigation agriculture but also for maintaining biodiversity due to its enrichment of aquatic flora and fauna (Imentai *et al.*, 2015). However, the whole basin is now facing several threats in the context of recent global warming trends and increasing human-induced pressure. For example, massive water use caused by the rapid development of irrigation agriculture will lead to significant water-level declines and subsequent unbearable salinization, which are disastrous for aquatic flora and fauna (Sala *et al.*, 2020a). The intensive use of agricultural fertilizers and massive industrial wastewater discharge will accelerate the lake eutrophication process (Imentai *et al.*, 2015). Reliable assessments of these threats and instructions for appropriate man-

agement strategies require understanding the history of environmental changes in the lake, as well as its responses to natural and anthropogenic stressors (Smol, 2019).

Paleolimnological methods based on multiple proxies in lake sediments can provide valuable information about environmental variation in lakes and their catchments (Brenner *et al.*, 1999; Batarbee and Bennion, 2011; Wu *et al.*, 2013; Liu *et al.*, 2017). Among the many proxies in lake sediments, *n*-alkanes and *n*-fatty acids have received the most attention due to their source-specific characteristics (Meyers, 2003). *n*-Alkanes can be biosynthesized by multiple producers, such as phytoplankton/algae (Cranwell *et al.*, 1987), aquatic macrophytes (Cranwell, 1984; Ficken *et al.*, 2000), land plants (Eglinton and Hamilton, 1967), and bacteria (Han and Calvin, 1969). The predominance of odd carbon numbers is a feature of biologically produced *n*-alkanes (Scalan and Smith, 1970), which can indicate certain biogenic origins owing to their source specificity (Meyers, 2003). It is widely accepted that bacteria and phytoplankton/algae are characterized by short-chain *n*-alkanes ($n\text{-C}_{15}\text{--}n\text{-C}_{20}$), aquatic macrophytes are the main producers of mid-chain *n*-alkanes ($n\text{-C}_{21}\text{--}n\text{-C}_{25}$), and terrestrial plants are commonly characterized by long-chain *n*-alkanes ($n\text{-C}_{26}\text{--}n\text{-C}_{35}$) (Eglinton and Hamilton, 1967; Cranwell *et al.*, 1987; Meyers, 2003). *n*-Fatty acids are another lipid biomarker for organic matter (OM) source tracing in sediments, and even-carbon chain lengths can indicate biological origins (Volkman *et al.*, 1998; Meyers, 2003). Lipid biomarkers are thus regarded as among the most effective indicators in lake sediments and are widely applied in paleoenvironmental investigations to distinguish between allochthonous (terrestrial plant-based) and autochthonous (phytoplankton-, algae- and macrophyte-based) sources of OM inputs, vegetation cover history in catchments (Schwark *et al.*, 2002), and anthropogenic impacts on terrestrial and aquatic ecosystems (Lu and Meyers, 2009; Fang *et al.*, 2017).

Previous studies on the Ili-Balkhash Basin have focused

mainly on evaluating recent environmental conditions, such as concentrations and distributions of persistent organic pollutants in water (Shen *et al.*, 2021a), spatial variations and controls on the hydrochemistry of surface water (Shen *et al.*, 2021b) and assessments of natural resources in the basin (Pueppke *et al.*, 2018a). Others have focused on environmental and climatic variability on a millennial scale (Chiba *et al.*, 2016; Mischke *et al.*, 2020). However, there are few continuous records documenting environmental and ecological variations and the responses to natural and anthropogenic impacts due to the limited scope and timespan covered by instrumental records. In this study, the abundance and composition of lipid biomarkers (including *n*-alkanes and *n*-fatty acids) in a ~200-year high-resolution sedimentary core from Lake Balkhash were analyzed to achieve the following objectives: i) identify potential sources and environmental significance of lipid biomarkers and trace their changes; ii) reveal the history of environmental changes in the Ili-Balkhash Basin over the past two centuries; and iii) determine the possible forces that drove those changes.

METHODS

Geographic setting and sampling

Lake Balkhash (approximately 73–80°N, 44–47°E; 342 m above sea level) is situated in southwest Kazakhstan and is now the largest water body in ACA (Fig. 1a). The lake is closed and slightly saline. The mean surface area of the lake is 17,000 km², and there is no surface outlet (Sala *et al.*, 2020). The water level of the lake has varied between 340.5 and 344.4 m in the past ~140 years under climatic and anthropogenic impacts. Approximately 84% of the lake's input water is derived from river inflows, and the Ili River is the most important contributor, supplying ca. 78% of the inflowing water to the lake (Sala *et al.*, 2020).

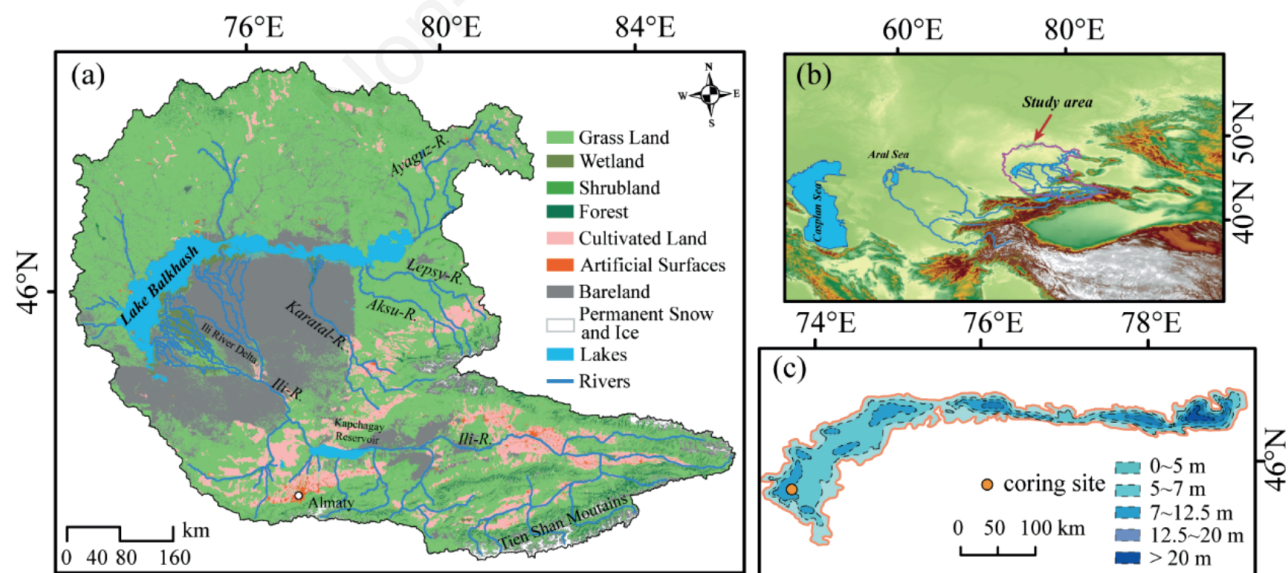


Fig. 1. a) Vegetation distribution of the Ili-Balkhash Basin, the land use data were obtained from the GlobeLand 30: <http://www.globallandcover.com/>. b) Location of the study area in Central Asia. c) Coring site and bathymetry of the lake (modified after Chiba *et al.*, 2016).

Lake Balkhash has a catchment area of 501,000 km² (Fig. 1b), and the catchment is characterized by an arid to semiarid climate, with a mean annual temperature of 17.5°C and a mean annual precipitation of 110 mm (Sala *et al.*, 2020). Under such dry conditions, natural ecosystems and agricultural activities (*e.g.*, irrigation farming and animal herding) in the region are largely dependent on water resources. The estuary delta formed by the Ili River, with an area of approximately 8000 km², is significant for the biodiversity of the region (Imentai *et al.*, 2015).

Because of the continental arid climate, the vegetation near the lake is composed of desert and steppe species, and riparian forests are commonly found in the lake shore area. The Ili Delta and shallow shore regions of the lake are densely covered by emergent plants (*e.g.*, *Phragmites*, *Typha* and *Scirpus*) (Imentai *et al.*, 2015). The common phytoplankton species in Lake Balkhash include dinoflagellates, diatoms, blue-green algae and green algae (Barinova *et al.*, 2017). The aquatic macrophytes (free-floating and submerged) in the lake are composed of the following species: *Lemna minor* (common duckweed), *Utricularia vulgaris* (common bladderwort) and *Ceratophyllum demersum* (hornwort) (Imentai *et al.*, 2015).

A 71-cm-long undisturbed sediment-water interface core (BLK) was collected in 2017 from the western zone of Lake Balkhash (45°41'N, 73°45'E; Fig. 1c) in 8 m of water using a gravity corer (Uwitec, Mondsee, Austria). Subsamples were taken at contiguous 1-cm intervals and refrigerated at -20°C prior to analysis.

¹³⁷Cs and ²¹⁰Pb dating

Ten-gram samples of the dried subsamples were sealed and stored at constant temperature and humidity for more than 30 days to maintain the radioactive equilibrium of ²²⁶Ra and ²¹⁰Pb. The ¹³⁷Cs and ²¹⁰Pb activities were determined by direct gamma spectrometry. The supported ²¹⁰Pb activity in each sample was assumed to be in equilibrium with the in situ ²²⁶Ra activity. The unsupported ²¹⁰Pb activity at each depth was calculated by subtracting the ²²⁶Ra activity from the total ²¹⁰Pb activity. The chronology models adopted for sediment dating were constructed with the serac package in the R software system (version 4.0.3; Bruel and Sabatier, 2020).

Extraction and analysis of lipid biomarkers

Sediment samples were Soxhlet-extracted for 24 h with a mixture of methylene chloride/methanol (v/v, 9:1) to obtain a total lipid extract after adding known quantities of internal standards. The mixture of extracts was saponified with 5% KOH-methanol solution by heating in a 100°C water bath. The neutral fraction was isolated by extraction with hexane and fractionated using silica gel column chromatography. The fatty acid (FA) fractions were isolated with hexane after acidification to pH 1 with 3 N HCl and then methylated with 14% BF₃/MeOH (60 C, 120 min) before being analyzed by gas chromatography-mass spectrometry (GC-MS). Molecular identification was conducted by GC-MS using an Agilent 5975 mass spectrometer coupled to an Agilent 7890A gas chromatograph with a DB-5MS column (30 m × 0.25 mm × 0.25 μm). The GC-MS oven temperature program for hydrocarbons was initiated at 80°C for 2 min and increased at a rate of 3°C min⁻¹ up to 300°C, after which the temperature was held for 20 min. To determine the FAs, the GC

oven temperature program started at 80°C (2 min), followed by an increase to 290°C at 4°C min⁻¹, after which the temperature was held for 15 min. The studied compounds were identified by comparison with previously reported mass spectra and interpretation of fragmentation patterns and chromatographic retention behavior. Quantification was conducted by comparing the peak areas of the studied compounds with that of the internal standard. Biomarker levels were normalized to total organic carbon content (μg g⁻¹ total organic carbon) to minimize the effect of varying sedimentation rates and degradation on biomarker content (Zhang *et al.*, 2021).

Determination of total organic carbon and total nitrogen

Before determination, the selected samples were treated with HCl to dissolve carbonate and then rinsed with distilled water to eliminate chloride. The total organic carbon (TOC) and total nitrogen (TN) concentrations were detected by a CE-440 elemental analyzer. The molar C/N ratio was calculated in the present study as follows: TOC/TN = (TOC/12)/(TN/14).

Calculation of biomarker indicators and statistical analyses

Several indices, *e.g.*, the carbon preference index for high molecular weight (CPIH) (Bray and Evans, 1961), the carbon preference index for low molecular weight (CPIL) (Cranwell *et al.*, 1987), and the proportion of aquatic macrophytes (Paq) (Ficken *et al.*, 2000), were applied to distinguish OM sources and infer environmental variation. The following equations were used for the calculations:

$$\text{CPIH} = 1/2 \times [(n\text{-C}_{25} + n\text{-C}_{27} + n\text{-C}_{29} + n\text{-C}_{31}) / (n\text{-C}_{24} + n\text{-C}_{26} + n\text{-C}_{28} + n\text{-C}_{30}) + (n\text{-C}_{25} + n\text{-C}_{27} + n\text{-C}_{29} + n\text{-C}_{31}) / (n\text{-C}_{26} + n\text{-C}_{28} + n\text{-C}_{30} + n\text{-C}_{32})] \quad (\text{eq. 1})$$

$$\text{CPIL} = (n\text{-C}_{15} + n\text{-C}_{17} + n\text{-C}_{19}) / (n\text{-C}_{16} + n\text{-C}_{18} + n\text{-C}_{20}) \quad (\text{eq. 2})$$

$$\text{Paq} = (n\text{-C}_{23} + n\text{-C}_{25}) / (n\text{-C}_{23} + n\text{-C}_{25} + n\text{-C}_{29} + n\text{-C}_{31}) \quad (\text{eq. 3})$$

$$\text{L-ALKs} = n\text{-C}_{27} + n\text{-C}_{29} + n\text{-C}_{31} + n\text{-C}_{33} \quad (\text{eq. 4})$$

$$\text{M-ALKs} = n\text{-C}_{23} + n\text{-C}_{25} \quad (\text{eq. 5})$$

$$\text{S-ALKs} = n\text{-C}_{15} + n\text{-C}_{17} + n\text{-C}_{19} \quad (\text{eq. 6})$$

$$\text{L-FAs} = n\text{-C}_{24} + n\text{-C}_{26} + n\text{-C}_{28} + n\text{-C}_{30} \quad (\text{eq. 7})$$

$$\text{S-FAs} = n\text{-C}_{16} + n\text{-C}_{18} + n\text{-C}_{20} + n\text{-C}_{22} \quad (\text{eq. 8})$$

where C_{*i*} represents the concentration of the *n*-alkane (odd) and *n*-fatty acid (even) with *i* carbon numbers.

To discriminate sources of lipid biomarkers and further interpret the associated environmental variability, principal component analysis (PCA) with varimax rotation was conducted with both *n*-alkane and *n*-fatty acid data (normalized) using the statistical program SPSS Statistics 26.0 (SPSS, Inc., Chicago, USA). An eigenvalue greater than one was selected to explain the percentage of the total variation among the parameters. Constrained incremental sum-of-squares clustering analysis (CONISS) based on the *vegan* and *rioja* packages in the R software system was also conducted to investigate the environmental evolution process and characteristics at different time periods (version 4.0.3; Juggins, 2015). The significance of the three phases identified was then confirmed by the broken stick model.

RESULTS

Chronology

The age-depth model of the BLK core was based on $^{210}\text{Pb}_{\text{ex}}$ and ^{137}Cs radionuclide determination. ^{137}Cs activity was first recorded at 22 cm, corresponding to the beginning of atmospheric nuclear weapons tests (1954 AD) (Appleby, 2001). We interpreted a ^{137}Cs peak at 17 cm as the record of the peak in global atmospheric thermonuclear weapon tests (GTWT) in 1964 AD (Lan *et al.*, 2020) and another ^{137}Cs peak at 8 cm as a potential record of the Chernobyl accident (1986 AD) (Fig. 2a; Garcia-Orellana *et al.*, 2006). The $^{210}\text{Pb}_{\text{ex}}$ activity in the BLK core ranged from 0.9 Bq kg^{-1} at 47 cm to 162.8 Bq kg^{-1} near the top and exhibited an exponential decreasing trend with depth (Fig. 2a). To acquire a more accurate chronology, we applied the constant rate supply (CRS), constant initial concentration (CIC) and piecewise constant rate supply (CRS_{PW}) age models to the core. According to the CRS and CIC models, we calculated that the sediment core from 47 to 1 cm covers 128 years (1890–2017 AD) and 98 years (1920–2017 AD), respectively. However, the results were inconsistent with both the ^{137}Cs time markers at the depths of 22 cm (1954 AD) and 17 cm (1964 AD), suggesting that the direct application of the CRS and

CIC models is inappropriate in our study. Therefore, the CRS_{PW} model was subsequently employed to obtain a reliable dating sequence (Appleby, 2001; Bruel and Sabatier, 2020), with two segments in the BLK core separated by a ^{137}Cs time marker in 1964 AD (17 cm in depth). According to the CRS_{PW} model, we calculated that the sediment core from 47 to 1 cm covers 146 years (1872–2017 AD) (Fig. 2b), and 22 cm corresponded to 1954 AD, which was consistent with the time marker of ^{137}Cs appearance. The chronology of sediments below 47 cm was extrapolated using the average sedimentation rate (0.30 cm a^{-1}) between the depths of 22 and 47 cm. The bottom of the sediment core (71 cm) was assigned to ca. 1800 AD (Fig. 2b). Notably, the $^{210}\text{Pb}_{\text{ex}}$ activity in this study did not show a strict exponential decline with depth ($R^2=0.70$), which may influence the sediment age estimated from the radioisotope data. However, the objective of this study was to focus on reconstructing the main evolutionary stages of the environment over the past two centuries instead of estimating the exact timing of environmental and ecological changes, and the chronology of the studied core seems to be adequate.

Bulk organic matter parameters

The TOC and TN contents ranged from 0.78% to 1.69% and 0.08% to 0.14%, respectively, and exhibited similar patterns in

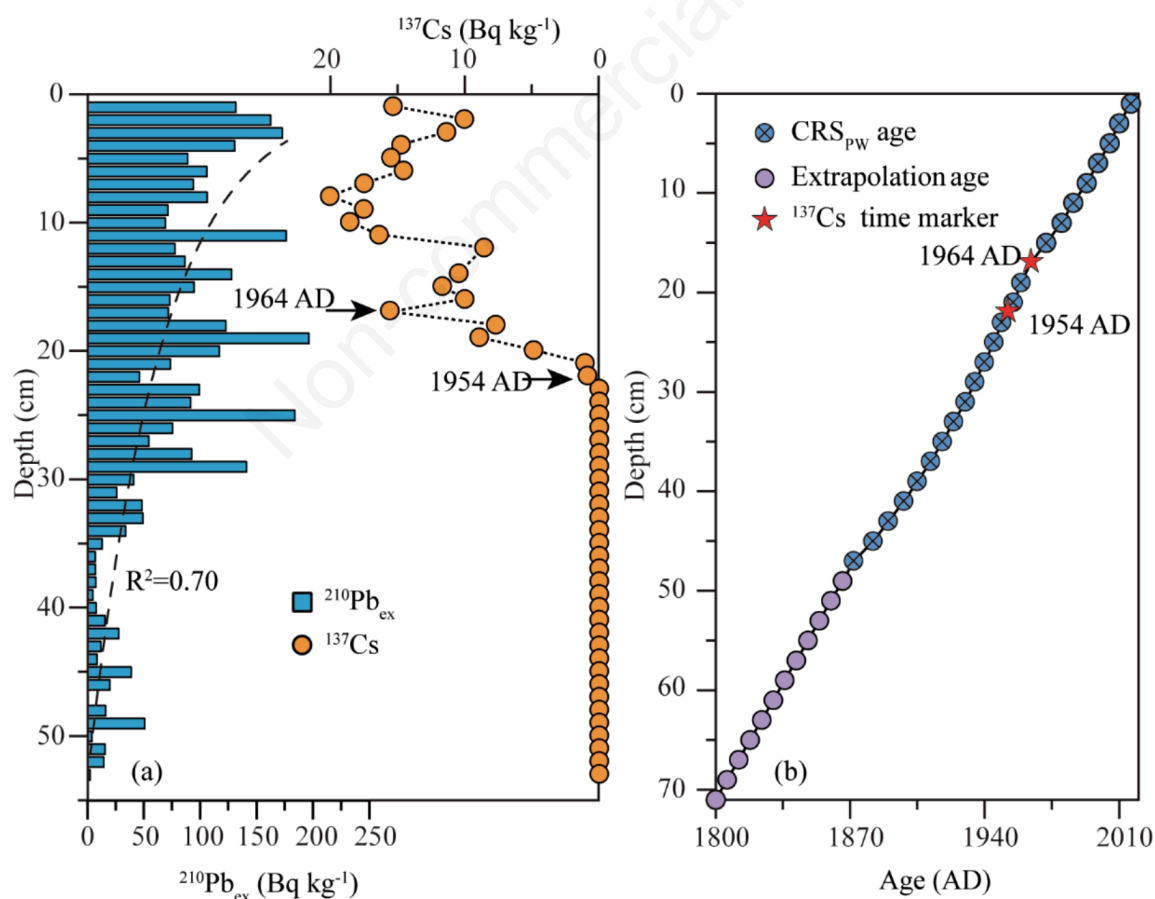


Fig. 2. The geochronology of BLK core for Lake Balkhash. a) Activities of $^{210}\text{Pb}_{\text{ex}}$ and ^{137}Cs versus sediment depth. b) Age-depth model calculated from ^{210}Pb CRS_{PW} model and ^{137}Cs .

the BLK core (Fig. 3), with the lowest concentrations occurring before 1860 AD and the highest concentrations occurring during 1860–1930 AD. Following a period of relatively low levels occur-

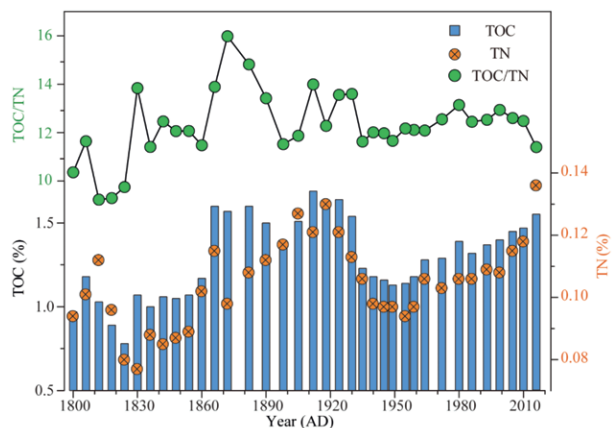


Fig. 3. Variation in TOC, TN and TOC/TN from the BLK core.

ring between 1930 and 1959 AD, the TOC and TN contents showed an increasing trend toward the core top, and the TN content displayed a more pronounced acceleration after 2000 AD (Fig. 3). The TOC/TN ratio ranged from 9.2 to 16.0 (averaged at 12.3) and fluctuated significantly before 1930 AD, with lower levels occurring during 1800–1860 AD and the highest levels occurring during 1860–1930 AD (Fig. 3). During 1930–2017 AD, the TOC/TN ratio remained relatively stable, except for a declining trend in more recent sediments (2000–2017 AD) (Fig. 3).

Distribution patterns of *n*-alkanes and *n*-fatty acids

On average, the *n*-alkanes in samples from the BLK core were characterized by a bimodal distribution, with chain lengths ranging from *n*-C₁₅ to *n*-C₃₃. Long-chain homologs ($\geq n$ -C₂₇) of *n*-alkanes showed a strong odd-over-even predominance throughout the sediment core, whereas short- and middle-chain length parts ($< n$ -C₂₇) displayed an even-carbon predominance (Fig. 4a). In contrast to that of *n*-alkanes, the average *n*-fatty acids distribution exhibited a unimodal pattern, with homologs ranging from *n*-C₁₆ to *n*-C₃₀, and displayed a strong even-carbon predominance (Fig. 4b). The variations in predominant *n*-alkanes and *n*-fatty acids

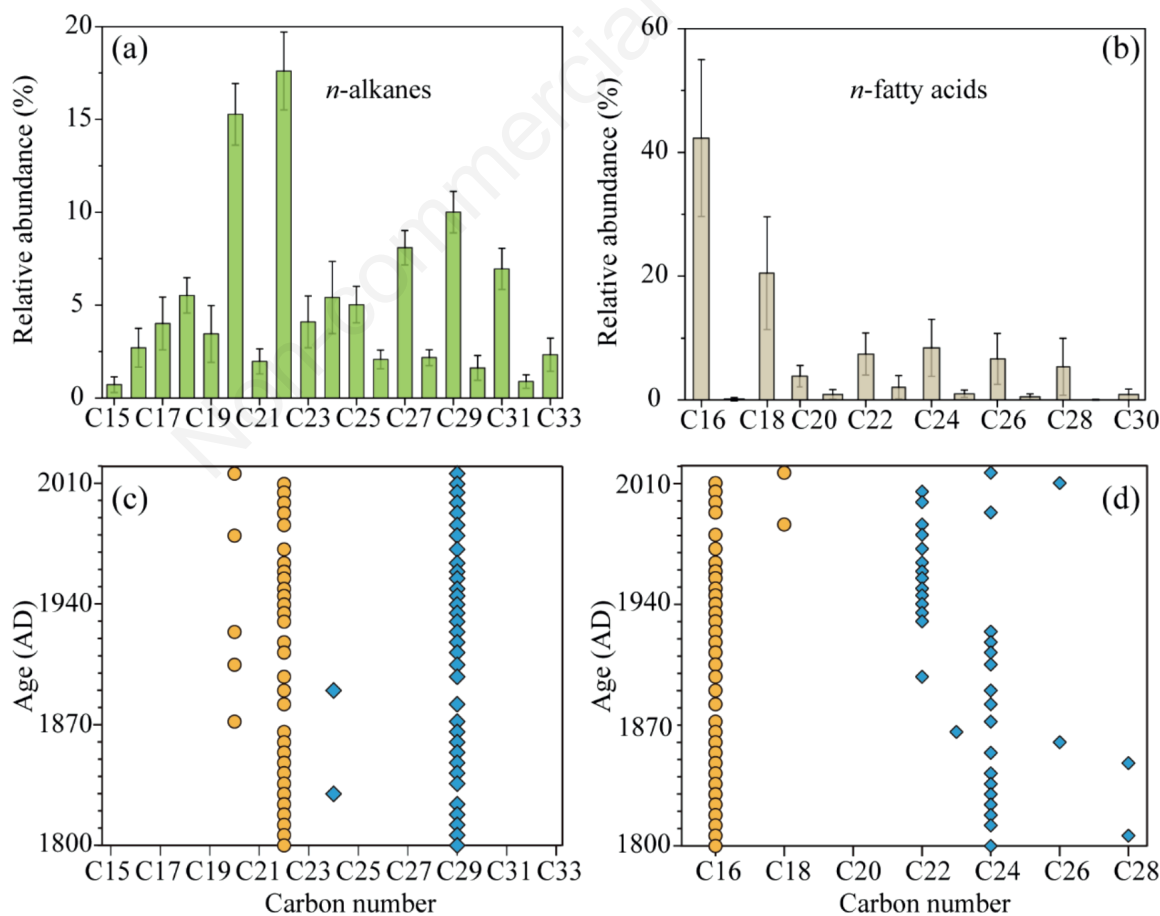


Fig. 4. Carbon molecule composition characteristics and Cmax of *n*-alkanes and *n*-fatty acids in BLK core. a) Carbon length distribution of *n*-alkanes. b) Carbon length distribution of *n*-fatty acids. c) Cmax profiles of *n*-alkanes. d) Cmax profiles of *n*-fatty acids.

(C_{\max}) throughout the core are shown in Fig. 4c and 4d. In most samples, $n-C_{29}$ was the predominant n -alkane of long-chain homologs ($\geq n-C_{27}$), except for two samples (43 and 61 cm) in which $n-C_{24}$ dominated (Fig. 4c). Mid- and short-chain n -alkanes ($\leq n-C_{27}$) rarely exhibited C_{\max} values at either $n-C_{22}$ or $n-C_{20}$ (Fig. 4c). Short-chain homologs of n -fatty acids ($\leq n-C_{20}$) were dominated by $n-C_{16}$ in most sediment samples. Long-chain homologs of n -fatty acids ($> n-C_{20}$) exhibited C_{\max} values at $n-C_{24}$ and $n-C_{22}$ in most sediment samples and occasionally at $n-C_{28}$, $n-C_{26}$ and $n-C_{23}$ in a few samples. Notably, the C_{\max} of long-chain homologs of n -fatty acids generally exhibited two distinct intervals, with $n-C_{24}$ dominating in pre-1930 sediment samples and $n-C_{22}$ dominating in after-1930 samples (Fig. 4d).

Concentrations of individual n -alkanes and n -fatty acids

Considering the principle that biogenic-sourced n -alkanes and n -fatty acids generally exhibit odd and even carbon preferences, respectively (Meyers, 2003), we mainly focused on odd-carbon n -alkanes and even-carbon n -fatty acids in the studied core. In addition, $n-C_{22}$ and $n-C_{20}$ alkanes, which significantly contributed to

the n -alkane profile, were also included. The variations in individual n -alkanes and n -fatty acids are shown in Fig. 5. Concentrations of $n-C_{15}$, $n-C_{17}$ and $n-C_{19}$ alkanes (short-chain) were generally low, averaging 0.03 , 0.15 and $0.13 \mu\text{g g}^{-1}$ TOC, respectively. Abundance variations in $n-C_{15}$ and $n-C_{17}$ alkanes exhibited a similar pattern, with low levels occurring during 1800–1920 AD, increased levels occurring during 1920–1970 AD, and a low level occurring during 1970–1990 AD, and an increasing trend occurring during 1990–2017 AD. $n-C_{19}$ alkanes exhibited relatively high levels during 1800–1970 AD and then a lower level during 1970–1990 AD. The abundance of $n-C_{19}$ alkanes also exhibited an increasing trend during 1990–2017 AD. $n-C_{20}$ and $n-C_{22}$ alkanes yielded relatively high concentrations averaging 0.56 and $0.65 \mu\text{g g}^{-1}$ TOC, respectively, and displayed a similar variation pattern, with generally lower levels occurring before 1930 AD and markedly increased values recorded during the period 1930–2017 AD. In addition, two synchronous concentration peaks of $n-C_{20}$ and $n-C_{22}$ were observed during 1898–905 AD and 1935–1959 AD. The concentrations of $n-C_{21}$, $n-C_{23}$ and $n-C_{25}$ alkanes (mid-chain) averaged 0.07 , 0.15 and $0.18 \mu\text{g g}^{-1}$ TOC, respectively. The $n-C_{23}$

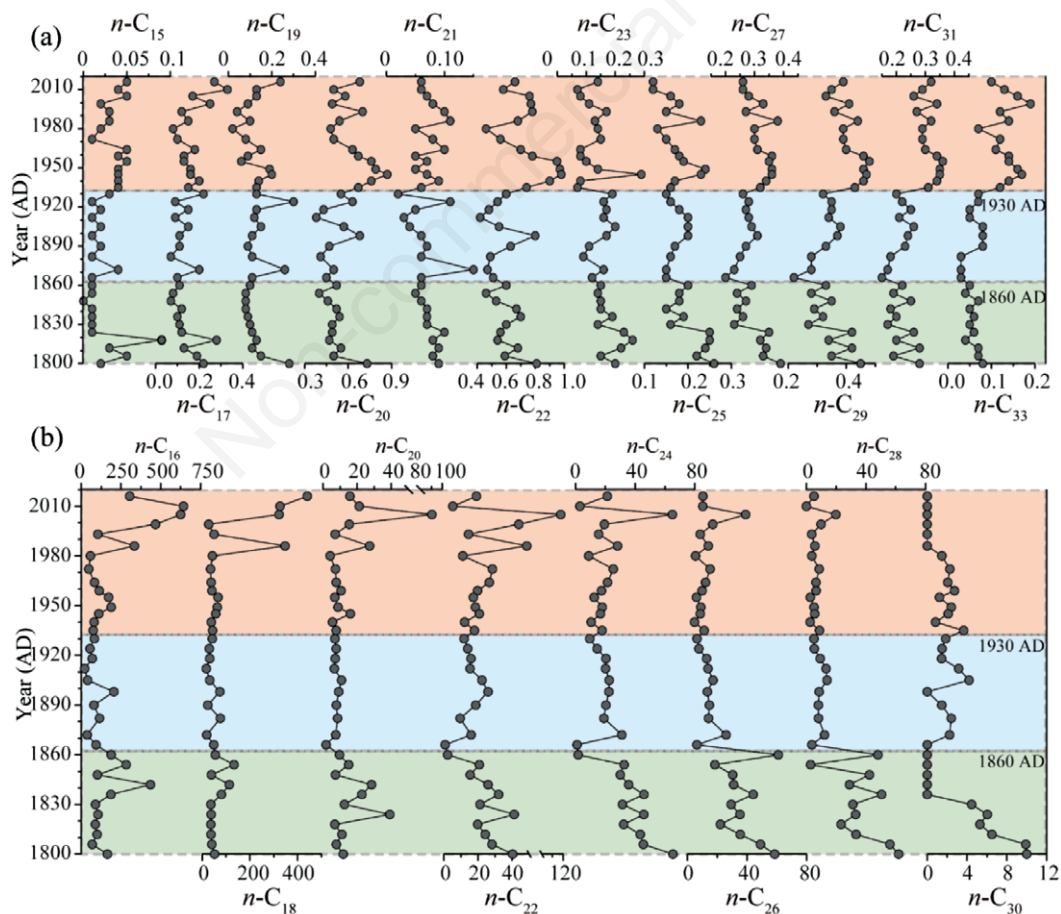


Fig. 5. The variations in individual n -alkanes ($\mu\text{g g}^{-1}$ TOC) and n -fatty acids ($\mu\text{g g}^{-1}$ TOC) concentration from the BLK core. a) Variations in individual n -alkane concentrations. b) Variations in individual n -fatty acid concentrations.

total variance and yielded high loadings on n -C₂₃ and n -C₂₅ alkanes and n -C₂₄, n -C₂₆, n -C₂₈ and n -C₃₀ fatty acids. PC3 and PC4 explained 16.8% and 8.8%, respectively, of the total variance, with the most positive loadings on n -C₁₆, n -C₁₈, n -C₂₀, and n -C₂₂ fatty acids and on n -C₁₅, n -C₁₇, and n -C₁₉ alkanes.

Based on the PCA, we conducted a CONISS on the scores of each PC to investigate the environmental evolution process and characteristics during different periods. Three distinct phases (1800-1860 AD, 1860-1930 AD, and 1930-2017 AD) were identified, as shown in Fig. 6c. The three distinct phases were clearly distinguished by the PC1-PC2 coordinate system (Fig. 6d). Sediment samples generally yielded high PC2 scores during the period 1800-1860 AD and were characterized by high PC1 scores in the period 1930-2017 AD, whereas 1860-1930 AD had low PC1 and PC2 scores.

DISCUSSION

Sources and environmental significance of lipid biomarkers

Lipid biomarkers in lake sediments originate primarily from plants living in lakes and the surrounding areas and from microorganisms in the water column. Variations in their abundance and composition could provide important information about possible sources and environmental changes despite their rather small proportion of total OM (Meyers, 2003). In this study, the PCA results showed that the n -C₂₀, n -C₂₂, n -C₂₇, n -C₂₉, n -C₃₁ and n -C₃₃ alkanes clustered together and yielded high positive loadings on PC1, which indicates that those components probably have a common source (Fig. 6a). Generally, long-chain n -alkanes (n -C₂₇, n -C₂₉, n -C₃₁ and n -C₃₃, L-ALKs) in lake sediments are commonly regarded to be derived from land plant leaf wax. Moreover, long-chain homologs of the n -alkane group in the BLK core were

maximized at n -C₂₉ and showed a strong odd carbon advantage (Fig. 4a), which is a common feature of long-chain n -alkanes originating from leaf wax constituents of terrestrial plants (Eglinton and Hamilton, 1967). The CPIH is a valuable proxy for determining n -alkane sources, with those of terrestrial plant origin generally exhibiting CPIH > 4 and those of petroleum origin displaying CPIH closer to 1 (Freeman and Pancost, 2014). Generally, the CPIH values obtained in this study averaged 3.7, indicating that the long-chain n -alkanes in the BLK core mainly originated from terrestrial plants in the catchment (Fig. 7a). Two intervals with relatively lower CPIH values (1800-1860 AD and 1980-2017 AD) indicated fewer terrestrial signals during these periods (Fig. 7a). Therefore, variations in long-chain n -alkanes and associated proxies may serve as effective indicators of terrestrial plants. Notably, the n -alkane profile in our core displays an unusual pattern in the n -C₁₂- n -C₂₂ range, with the predominant n -alkane being either n -C₂₀ or n -C₂₂ throughout the core (Fig. 4c). Previous investigators have documented the unusual distribution of n -alkane profiles in the n -C₁₂- n -C₂₂ range, with strong maxima of one or two even-numbered n -alkanes, and attributed this pattern to inputs from microorganisms inhabiting the water column (Affouri and Sahraoui, 2017; Wan *et al.*, 2018). Considering the close connection between n -C₂₀ and n -C₂₂ and terrestrial plant-derived n -alkanes, it is reasonable to attribute the differences in n -C₂₀ and n -C₂₂ to the microbial reworking of terrestrial OM.

Aquatic macrophyte-derived n -alkanes are often dominated by mid-chain homologs (Ficken *et al.*, 2000), such as n -C₂₃ and n -C₂₅ (M-ALKs), which are grouped together with n -C₂₄, n -C₂₆, n -C₂₈ and n -C₃₀ fatty acids (L-FAs) and have high positive loadings on PC2, indicating that those components mainly originated from aquatic macrophytes. Typically, Paq values vary distinctly when n -alkanes are derived from terrestrial plants (<0.1), emergent macrophytes (0.1-0.4) or submerged/floating macrophytes (>0.4) (Ficken *et al.*, 2000). In agreement with these findings,

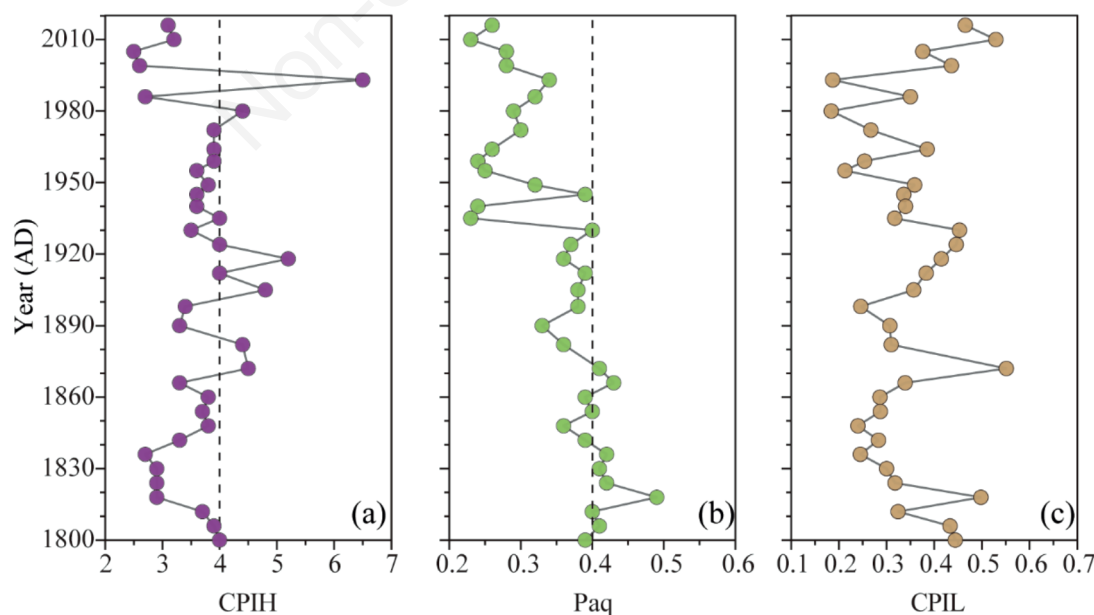


Fig. 7. Diagnostic ratios of biomarker source identification from the BLK core. a) CPIH. b) Paq. c) CPIL.

the Paq values in this study averaged 0.35, reflecting the significant contribution of aquatic macrophytes, especially in the period 1800–1860 AD, which yielded higher Paq values averaging 0.41 (Fig. 7b). Previous investigations revealed that aquatic macrophytes can produce abundant long-chain *n*-fatty acids, especially *n*-C₂₄ and *n*-C₂₆ homologs (Ficken *et al.*, 2000; Liu and Liu, 2017). In agreement with these findings, *n*-C₂₄ and *n*-C₂₆ fatty acids exhibited relatively high abundances in the *n*-C₂₀–*n*-C₃₀ range (Fig. 4b). The CPIL is commonly used to determine the origin of *n*-alkanes in the *n*-C₁₅–*n*-C₂₀ range. Petroleum-derived *n*-alkanes yielded CPIL values close to 1.0, while *n*-alkanes of phytoplankton and aquatic photosynthetic bacteria origin are typically dominated by odd-carbon-number compounds (*n*-C₁₅, *n*-C₁₇ and *n*-C₁₉), with CPIL > 1.0 (Cranwell *et al.*, 1987). For example, *n*-C₁₇ and *n*-C₁₉ are commonly thought to be cyanobacterial in origin (Santos Neto *et al.*, 1998). Non-photosynthetic bacteria in the water column are also significant producers of *n*-alkanes in the *n*-C₁₅–*n*-C₂₀ range and are usually dominated by even-carbon compounds, with maxima occurring at *n*-C₁₆, *n*-C₁₈ or *n*-C₂₀ and CPIL < 1.0. In this study, the relatively low CPIL values (<1.0) reflected relatively strong microbial activity in the water column, which was consistent with the high concentrations of *n*-C₂₀ and *n*-C₂₂ alkanes (Figs. 7c and 4a). Odd-carbon-number *n*-alkanes (*n*-C₁₅, *n*-C₁₇ and *n*-C₁₉, S-ALKs) in the *n*-C₁₅–*n*-C₂₀ range were clustered together with high loadings on PC3 in this study (Fig. 6b), indicating a typical phytoplankton origin feature and providing valuable information about variations in phytoplankton biomass in the lake ecosystem. Short-chain *n*-fatty acids (*n*-C₁₆, *n*-C₁₈, *n*-C₂₀, *n*-C₂₂, S-FAs) were clustered together and constituted the main components of PC4 (Fig. 6b). In general, *n*-C₁₄–*n*-C₁₈ fatty acids are reported to be the dominant lipid components of phytoplankton, algae and bacteria. For example, *n*-C₁₈ predominates in green algae, and *n*-C₁₆ is abundant in diatoms and cyanobacteria (Volkman *et al.*, 1998). Therefore, these components were also closely associated with phytoplankton algae and bacteria. However, short-chain *n*-alkanes and *n*-fatty acids were not clustered together and exhibited different variation trends throughout the core, as displayed in Figs. 5 and 6b. This discrepancy could be attributed to two main reasons. First, short-chain *n*-fatty acids are generally regarded as ubiquitous components of biota that are less source specific than other compounds and may obscure their origin. In addition, short-chain *n*-fatty acids are more susceptible to degradation and modification than short-chain *n*-alkanes are, especially in older sediments deposited in the lower part of the core, which could explain both the higher concentration levels of short-chain *n*-alkanes and *n*-fatty acids in more recent sediments (*e.g.*, deposited in 1990–2017 AD). This discrepancy may indicate that short-chain *n*-alkanes and *n*-fatty acids had different source organisms before the 1980s according to their abundance variations (Fig. 5). A previous study conducted in Lake Balkhash revealed that diatoms dominate in spring and autumn, green algae dominate during periods of increasing temperature, and blue–green algae dominate in summer (Mischke, 2020). A possible explanation was that short-chain *n*-alkanes were mainly contributed by diatoms before the 1980s because the lake was oligotrophic and because the regional temperatures were relatively low. In recent decades, green algae and cyanobacteria that prefer higher temperatures may be the common sources of both short-chain *n*-alkanes and *n*-fatty acids as a result of marked in-

creases in regional temperature and nutrient levels in the lake (Moberg *et al.*, 2005; Krupa *et al.*, 2020).

Environmental change and its possible driving force in the Ili-Balkhash Basin since 1800 AD

Temporal variations in sedimentary biomarkers in the BLK core reveal three main historical phases of environmental change in the Ili-Balkhash Basin over the past ~200 years. To describe the environmental characteristics of each phase and further discuss possible driving forces, we compared our results with climate data and historical records in the region.

Phase I (1800–1860 AD)

In this phase, the evidence presented herein indicates a high-water-level lake system with abundant aquatic macrophytes (submerged and floating) and an overall minor terrestrial signal. The higher abundance of M-ALKs and higher Paq ratios suggest that aquatic macrophytes were abundant and were a dominant contributor to the organic component of the sediment record (Fig. 8 b,c), which likely indicates that the lake was in a clear-water status during this period (Toivonen and Huttunen, 1995). A higher L-FA abundance coupled with a lower TOC/TN ratio (average 13.1) recorded in this phase further confirm that aquatic macrophytes were dominant (Fig. 8 e,h). This is also supported by the *n*-fatty acid C_{max} that typically occurs at aquatic macrophyte-derived *n*-C₂₄ during this phase (Fig. 4d). In turn, evidence presented by a lower abundance of S-ALKs and S-FAs suggests limited overall phytoplankton productivity in the lake during this period (Fig. 8 d,f). This interpretation, coupled with the aquatic proxies (*e.g.*, Paq and L-FAs), suggests a high-water-level and relatively clear lake with good light penetration that allows dense aquatic macrophytes and a minor phytoplankton state during this phase. A previous paleolimnological study revealed that the ostracod assemblage in the sediments deposited ca. 1757–1880 AD was dominated by *Ilyocypris spp.*, *L. inopinata*, *C. torosa* and *N. neglecta*, suggesting a lower salinity and higher water level (Mischke *et al.*, 2020), which provides strong evidence supporting our interpretations. In addition, according to the data estimated by former Soviet Union experts, the water level was much higher in 1840 AD (Propastin, 2012). This period was during the Little Ice Age (LIA; from ~1500 to 1850 AD) in ACA and was generally associated with wet conditions revealed by numerous studies (Chen *et al.*, 2010; Aichner *et al.*, 2015), which may offer a reasonable explanation for generally high lake levels during this phase.

Overall, a minor terrestrial signal in this phase is suggested by the low abundance of L-ALKs (Fig. 8a), from which a period with generally dense catchment vegetation cover may be inferred. Relatively wet conditions during this phase may promote the growth of vegetation in the catchment and prevent soil erosion, thus permitting overall limited terrestrial inputs. Further evidence to support this deduction includes pollen data, from which a period with relatively higher concentrations was detected ca. 1800–1890 AD (Feng *et al.*, 2013), and geochemical evidence of relatively low and stable concentrations of terrestrial materials represented by conservative elements, *e.g.*, Al, Ti and K (Huang *et al.*, 2020). Despite low terrestrial inputs, two fluctuations with relatively higher levels occurring in the periods 1800–1818 AD and 1848–1860 AD were still recorded (Fig. 8a, gray bars). Inter-

estingly, by comparison with reconstructed runoff from the Ili River (Panyushkina *et al.*, 2018), we found that the periods of higher terrestrial input corresponded to those of higher runoff (Fig. 8i). In general, the transport of leaf waxes to lake sediments involves three primary modes: direct deposition of leaf litter, aerosol deposition and surface flow carrying soil OM (often containing

terrestrial plant residues) (Diefendorf and Freimuth, 2017). Which mechanism prevails depends on the lake setting. In this study, surface flow is likely the primary mode for the following reasons. First, the Ili River, as the most significant contributor to the inflow of water to Lake Balkhash, supplies ca. 78% of the inflowing water to the lake and subsequently exerts considerable influence on the transport of land-derived debris. Moreover, the sampling site of the BLK core is close to the mouth of the Ili River and is likely susceptible to the impact of inflowing rivers. In addition, land-derived long-chain lipids are more likely to be transported to lakes via surface runoff under conditions of greater precipitation, which was demonstrated by an investigation conducted in the Issyk-Kul Basin (Zhang *et al.*, 2021). Therefore, synchronous fluctuations in terrestrial inputs and reconstructed runoff during this phase highlight that hydrological variability is an essential factor influencing the delivery process of terrestrial material.

Phase II (1860–1930 AD)

Phase II was associated with the gradual degradation of submerged/floating macrophytes and the increasing importance of emergent plants and terrestrial inputs. Overall, the decreases in aquatic proxy (Paq and L-FAs) values suggest that there were fewer submerged/floating macrophytes in this phase than in Phase I (Fig. 8 c,e), which may have been driven by periodic variations in water levels during this phase. A previous study indicated that the lake experienced the most significant water level change during this period (Propastin, 2012; Sala *et al.*, 2020). Such a significant variation in water level is likely to inhibit the growth of submerged/floating macrophytes. Furthermore, decreased water levels provide abundant habitat for emergent plants, leading to an increasing contribution of emergent plants (vascular plants) to sedimentary organic records. This is supported by moderate Paq values (average of 0.38), suggesting that emergent plants living on the shallow shoreline of the lake and in the Ili Delta (*e.g.*, *Phragmites* and *Typha*) increase in importance in terms of contribution to the organic geochemical record (Fig. 8c). A decrease in lake level would also permit an increasing dominance of terrestrial inputs, as reflected by the increasing trend in L-ALK concentrations (Fig. 8a), although terrestrial inputs are also low (with values similar to those observed in Phase I). The deduction of an expansion of terrestrial and emergent plants was also evidenced by the highest TOC and TOC/TN ratio in this phase (Fig. 8 g,h). Similar to the previous stage, in the 1890–1905 AD, the synchronous peaks in terrestrial inputs and reconstructed runoff also emphasize that higher runoff promoted the delivery of terrestrial material (Fig. 8 a,i; gray bar). In addition, additional terrestrial inputs partly override the M-ALK signal (submerged/floating macrophytes) because land plant leaf wax also contains a large amount of M-ALKs, which may offer a reasonable explanation for the discrepant trend between M-ALKs and other aquatic proxies (*e.g.*, Paq, L-FAs). In turn, phytoplankton productivity was also generally limited compared to that in the previous phase, except at the end of this phase (1924–1930 AD), as reflected by an increase in S-ALKs (Fig. 8d). Additionally, it is worth noting that S-ALKs appear to reflect a phytoplankton bloom in the 1870s (Fig. 8d), which may be attributed to the extremely low water level, as revealed by both the water level record and reconstructed runoff (Fig. 8i; Propastin, 2012). A possible mechanism is that lower lake levels lead to occasional mixing of nutrient-rich deeper waters, providing an internal source of nutrients that may have resulted

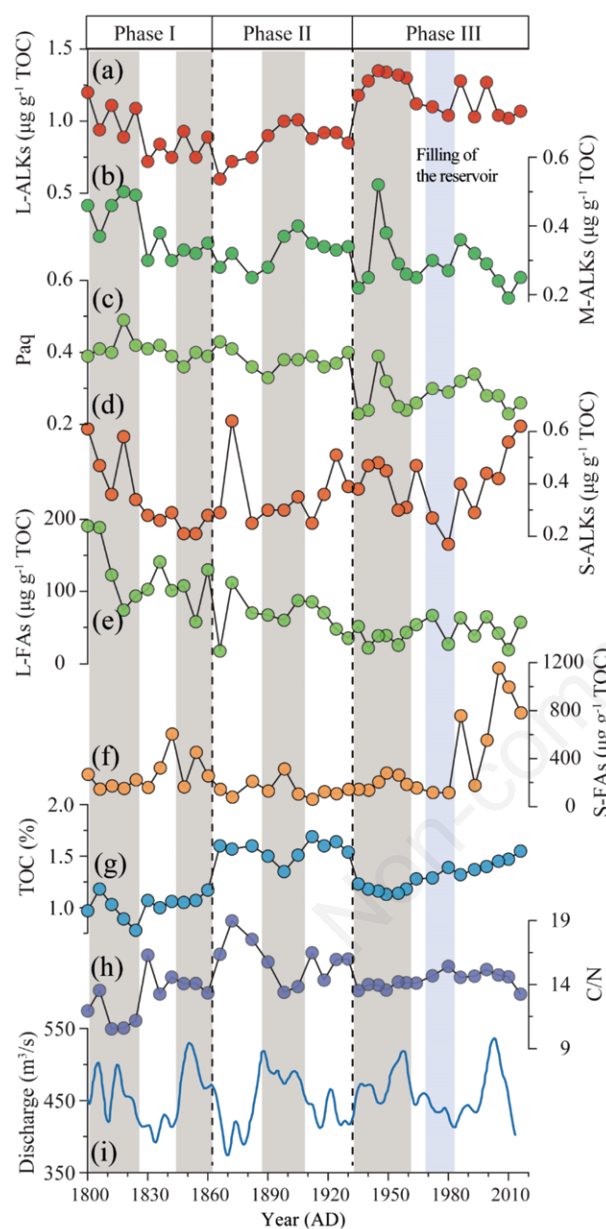


Fig. 8. Biomarker records indicative of environmental changes at Lake Balkhash over the last ~200 years. a) Long-chain *n*-alkanes (L-ALKs). b) Mid-chain *n*-alkanes (M-ALKs). c) Proportion of aquatic macrophytes (Paq). d) Short-chain *n*-alkanes (S-ALKs). e) Long-chain *n*-fatty acids (L-FAs). f) Short-chain *n*-fatty acids (S-FAs). g) TOC contents. h) TOC/TN. i) Reconstructed discharge in the Ili River (Panyushkina *et al.*, 2018). The gray bars indicate periods with high terrestrial inputs and blue bar indicates the period of filling of the Kapchagay Reservoir.

in a phytoplankton bloom (Mills *et al.*, 2018). Therefore, during Phase II, Lake Balkhash experienced a decrease in the cover of submerged/floating macrophytes and an expansion in that of emergent plants compared to those in the previous phase.

Phase III (1930-2017 AD)

The final phase was a period associated with strong disturbance in the catchment and could mainly be attributed to increasing anthropogenic impacts. The most striking feature of this phase is the significantly increased contribution of terrestrial inputs to the lake compared to that in the previous phases, with L-ALK abundance being the highest on record during 1935–1959 AD (Fig. 8a). Terrestrial material mobilization to aquatic systems is largely promoted by anthropogenic catchment alteration, and evidence is widespread, such as in records from Lake Nyamogusigiri (Mills *et al.*, 2018), Lake Murten (Haas *et al.*, 2020) and Lake Skottenesjön (Yang *et al.*, 2021). The impact may be acute, particularly in ACA. An extremely uneven rainfall distribution often leads to heavy seasonal rainfall, which facilitates transport, delivering large amounts of land-derived material to lakes, especially in arid regions with loose soil and sparse vegetation cover. According to historical documents, 1935-1959 AD corresponds to the beginning of large-scale exploitation in Central Asia supported by the former Soviet Union, associated with the rapid development of reclaimed agriculture and the livestock industry in the Ili-Balkhash Basin (Propastin, 2012; Pueppke *et al.*, 2018b), which likely resulted in widespread soil disturbance and exposure of more plant residues. Moreover, the logging and utilization of terrestrial vegetation, such as *Phragmites australis* (an important fodder plant) and *H. aphyllum* (fuel wood), by local people may also lead to enhanced soil erosion and the production of more terrestrial material (Imentai *et al.*, 2015). More terrestrial material coupled with the higher reconstructed runoff of the Ili River led the highest terrestrial inputs on record during this time (Fig. 8a, i). Interestingly, there was an anti-correlation between the TOC/TN values and the reconstructed runoff from the Ili River, which may have been caused by elevated inputs of phytoplankton-derived OM (protein-rich) as the result of the increased nutrient loads delivered by river inflows. In agreement with these findings, the high river discharge basically corresponded to the high contents of S-ALKs and S-FAs (such as during 1800-1820 AD and 1930-1960 AD) (Fig. 8 d,f,i).

Several of the indicators (*e.g.*, M-ALKs and L-FAs) presented herein suggest that submerged/floating macrophytes were at their lowest levels on record during Phase III (Fig. 8 b,e). This is also supported by the lowest Paq values (average of 0.28), from which a significant contribution by emergent plants can be further inferred (Fig. 8c). These changes may be driven by further decreases in water levels and increasing salinity during this phase (Propastin, 2012; Myrzakhmetov *et al.*, 2017). The overall status of the aquatic proxies (*e.g.*, Paq and L-FAs) remaining relatively stable during Phase III likely suggests that the modern aquatic macrophyte community had formed since the beginning of the phase (Fig. 8 c,e). In contrast, markedly elevated S-ALK values suggest that the lake experienced an increase in phytoplankton productivity during this phase (Fig. 8d). In particular, the period 1986-2016 AD was characterized by the rapid accumulation of short-chain lipids (S-ALKs and S-FAs) and an increase in TN content, suggesting that the lake has become an increasingly productive system in recent decades (Figs. 3 and 8 d,g). There are

three main probable reasons for the increasingly productive lake system. First, compared with that in the previous phases, the regional climate shifted to warmer conditions, especially after the 1980s (Moberg *et al.*, 2005), which would directly promote the growth of phytoplankton and bacteria (Bornette and Puijalon, 2011). Second, increased nutrient loading due to the massive deployment of chemical fertilizers in the catchment and the development of fisheries since the late 1920s and early 1930s may serve as another important trigger (Pueppke *et al.*, 2018a, 2018b). Moreover, the shrinkage of the submerged/floating macrophyte cover may provide better conditions for the growth of the phytoplankton community. This degradation in submerged/floating macrophyte cover accompanied by an increase in phytoplankton abundance is also reflected in the C_{max} of *n*-fatty acids switching from *n*-C₂₄ (aquatic macrophytes) to *n*-C₂₂ (phytoplankton) (Fig. 4d). Notably, aquatic material appears to remain the dominant contributor to sedimentary organic components, as suggested by the relatively low TOC/TN values (average 14.4) despite increased terrestrial inputs (Fig. 8h).

During this period, construction of the Kapchagay Reservoir on the Ili River in 1970 AD and the subsequent filling of the reservoir (1970-1988 AD) caused an ecological crisis for Lake Balkhash, leading to lake level decline, salinity rise and biodiversity loss, which have been revealed by many investigations (Krupa *et al.*, 2014; Imentai *et al.*, 2015; Mischke *et al.*, 2020). These significant changes were also recorded by the sedimentary biomarkers in our study. According to a previous study, the phytoplankton productivity in the western part of the lake decreased by 50% with increasing salinity in the 1970s (Krupa *et al.*, 2014), which was also reflected by the sharp decrease in the abundance of S-ALKs in this study (Fig. 8d, blue bar).

CONCLUSIONS

In this study, we examined the composition and abundance of sedimentary lipid biomarkers (*n*-alkanes and *n*-fatty acids) in the BLK core to discuss their environmental significance and further reveal the history of environmental evolution over the past two centuries. The two main conclusions are as follows: i) The application of both *n*-alkane and *n*-fatty acid profiles permitted better discrimination of sedimentary OM sources. Long-chain *n*-alkanes in the BLK core mainly represent terrestrial inputs, and both *n*-fatty acids and mid-/short-chain *n*-alkanes mainly contain aquatic signals. ii) Three distinct phases (1800–1860 AD, 1860–1930 AD and 1930–2017 AD) were identified. During Phase I (1800-1860 AD), Lake Balkhash was a high-water-level lake system with abundant aquatic macrophytes (submerged and floating) and minor phytoplankton. Overall, the minor terrestrial inputs suggest dense vegetation in the catchment as the result of wet conditions. Several synchronous fluctuations between terrestrial inputs and reconstructed runoff highlight that hydrological variability plays a crucial role in promoting the delivery of terrestrial material in the study area. The subsequent Phase II (1860-1930 AD) corresponds to a period featuring the decreased importance of submerged/floating macrophytes and the increasing importance of emergent plants and terrestrial inputs. A great variation in water levels likely led to the shrinkage of submerged/floating macrophyte cover. Phase III (1930-2017 AD) was characterized by the strong influence

of anthropogenic disturbances within the last ~200 years of the lake's history. The highest terrestrial inputs on record highlight intensive exploitation of the catchment during 1935-1959 AD. Increased human-induced nutrient loading coupled with elevated regional temperature prompted the lake to become an increasingly productive lake system. Submerged/floating macrophytes during this phase were at the lowest levels in response to the decreased water levels and increasing salinity.

ACKNOWLEDGMENTS

We thank the CAS Research Center for Ecology and Environment of Central Asia for assistance. We are also grateful to the reviewer for the helpful comments. The paper was supported by the National Natural Science Foundation of China (Grant No. U2003202; 41671200) and the Strategic Priority Research Program of the Chinese Academy of Sciences, Pan-Third Pole Environment Study for a Green Silk Road (Grant No. XDA2006030101).

REFERENCES

- Affouri H, Sahraoui O, 2017. The sedimentary organic matter from a Lake Ichkeul core (far northern Tunisia): Rock-Eval and biomarker approach. *J Afr Earth Sci* 129:248-259.
- Aichner B, Feakins SJ, Lee JE, Herzschuh U, Liu X, 2015. High-resolution leaf wax carbon and hydrogen isotopic record of the late Holocene paleoclimate in arid Central Asia. *Clim Past* 11:619-633.
- Appleby PG, 2001. Chronostratigraphic technique in recent sediments, p. 171-203. In: Last WL, Smol JP (eds.), *Tracking environmental change using lake sediments, volume 1: Basin analysis, coring, and chronological techniques*. Dordrecht: Kluwer Academic Publishers.
- Barinova S, Krupa E, Kadyrova U, 2017. Spatial dynamics of species richness of phytoplankton of Lake Balkhash in the gradient of abiotic factors. *Transylv Rev System Ecol Res* 19:1-18.
- Battarbee RW, Bennion B, 2011. Palaeolimnology and its developing role in assessing the history and extent of human impact on lake ecosystems. *J Paleolimnol* 45:399-404.
- Bornette G, Puijalon S, 2011. Response of aquatic plants to abiotic factors: a review. *Aquat Sci* 73:1-14.
- Bray EE, Evans ED, 1961. Distribution of *n*-paraffins as a clue to recognition of source rocks. *Geochim Cosmochim Acta* 22:2-15.
- Brenner M, Whitmore TJ, Lasi MA, Cable JE, Cable PH, 1999. A multi-proxy trophic state reconstruction for shallow Orange Lake, Florida, USA: possible influence of macrophytes on limnetic nutrient concentrations. *J Paleolimnol* 21:215-233.
- Bruel R, Sabatier P, 2020. *serac*: an R package for short-lived radionuclide chronology of recent sediment cores. *J Environ Radioact* 225:106449.
- Chen F, Chen JH, Homes J, Boomer I, Austin P, Gates JB, et al., 2010. Moisture changes over the last millennium in arid central Asia: A review, synthesis and comparison with monsoon region. *Quat Sci Rev* 29:1055-1068.
- Chiba T, Endo K, Sugai T, Haraguchi T, Kondo R, Kubota J, 2016. Reconstruction of Lake Balkhash levels and precipitation/evaporation changes during the last 2000 years from fossil diatom assemblages. *Quat Int* 197:330-341.
- Cranwell PA, 1984. Lipid geochemistry of sediments from Upton Broad, a small productive lake. *Org Geochem* 7:25-37.
- Cranwell PA, Eglinton G, Robinson N, 1987. Lipids of aquatic organisms as potential contributors to lacustrine sediments. *Org Geochem* 11:513-527.
- Diefendorf AF, Freimuth EJ, 2017. Extracting the most from terrestrial plant-derived *n*-alkyl lipids and their carbon isotopes from the sedimentary record: A review. *Org Geochem* 103:1-21.
- Eglinton G, Hamilton RJ, 1967. Leaf epicuticular waxes. *Science* 156:1322-1335.
- Fang J, Wu F, Xiong Y, Wang S, Yang H, 2017. A comparison of the distribution and sources of organic matter in surface sediments collected from northwestern and southwestern plateau lakes in China. *J Limnol* 76:1607.
- Feng ZD, Wu HN, Zhang CJ, Ran M, Sun AZ, 2013. Bioclimatic change of the past 2500 years within the Balkhash Basin, eastern Kazakhstan, Central Asia. *Quat Int* 311:63-70.
- Ficken KJ, Li B, Swain DL, Eglinton G, 2000. An *n*-alkane proxy for the sedimentary input of submerged/floating freshwater aquatic macrophytes. *Org Geochem* 31:745-749.
- Freeman KH, Pancost RD, 2014. Biomarkers for terrestrial plants and climate, p. 395-416. In: Turekian HD, Holland KK (eds.), *Treatise on geochemistry*. Amsterdam: Elsevier.
- Garcia-Orellana J, Gracia E, Vizcaino A, Masque P, Olid C, Martinez-Ruiz F, et al., 2006. Identifying instrumental and historical earthquake records in the SW Iberian Margin using ²¹⁰Pb turbidite dating. *Geophys Res Lett* 33:L24601.
- Haas M, Kaltenrieder P, Ladd SN, Welte C, Strasser M, Eglinton TI, Dubois N, 2020. Land-use evolution in the catchment of Lake Murten, Switzerland. *Quat Sci Rev* 230:106154.
- Han J, Calvin M, 1969. Hydrocarbon distribution of algae and bacteria, and microbiological activity in sediments. *PNAS* 64:436-443.
- Huang K, Ma L, Abuduwaili J, Liu W, Issanova G, Saparov G, Lin L, 2020. Human-induced enrichment of potentially toxic elements in a sediment Core of Lake Balkhash, the largest Lake in Central Asia. *Sustainability* 12:4717.
- Imentai A, Thevs N, Schmidt S, Nurtazin S, Salmurzauli R, 2015. Vegetation, fauna, and biodiversity of the Ile Delta and southern Lake Balkhash - A review. *J Great Lakes Res* 41:688-696.
- Juggins S, 2015. *rioja*: Analysis of Quaternary Science Data. R package version 0.9-9. Available from <http://cran.r-project.org/package=rioja>
- Krupa E, Slyvinskiy G, Barinova S, 2014. The effect of climatic factors on the long term dynamics of aquatic ecosystems of the Balkhash Lake (Kazakhstan, Central Asia). *Adv Stud Biol* 6:115-136.
- Lan JH, Wang TL, Chawchai S, Cheng P, Zhou K, Yu KK, et al., 2020. Time marker of ¹³⁷Cs fallout maximum in lake sediments of Northwest China. *Quat Sci Rev* 241:106413.
- Liu H, Liu WG, 2017. Concentration and distributions of fatty acids in algae, submerged plants and terrestrial plants from the northeastern Tibetan Plateau. *Org Geochem* 113:17-26.
- Liu W, Ma L, Wu JL, Abuduwaili JLL, 2017. Environmental variability and human activity over the past 140 years

- documented by sediments of Ebinur Lake in arid central Asia. *J Limnol* 76:1587.
- Lu YH, Meyers PA, 2009. Sediment lipid biomarkers as recorders of the contamination and cultural eutrophication of Lake Erie, 1909-2003. *Org Geochem* 40:912-921.
- Meyers PA, 2003. Applications of organic geochemistry to paleolimnological reconstructions: a summary of examples from the Laurentian Great Lakes. *Org Geochem* 34:261-289.
- Mills K, Vane CH, Lopes dos Santos RA, Ssemmanda I, Leng MJ, Ryves DB, 2018. Linking land and lake: using novel geochemical techniques to understand biological response to environmental change. *Quat Sci Rev* 202:122-138.
- Mischke S, 2020. Large Asian lakes in a changing world: natural state and human impact. Cham: Springer.
- Mischke S, Zhang CJ, Plessen B, 2020. Lake Balkhash (Kazakhstan): Recent human impact and natural variability in the last 2900 years. *J Great Lakes Res* 46:267-276.
- Moberg A, Sonechkin DM, Holmgren K, Datsenko NM, Karlén W, Lauritzen SE, 2005. Highly variable Northern Hemisphere temperatures reconstructed from low- and high-resolution proxy data. *Nature* 433:613-617.
- Myrzakhmetov A, Alimkulov S, Madibekov A, 2017. Level regime of Balkhash Lake as the indicator of the state of the environmental ecosystems of the region. *Int J Adv Res Sci Eng Technol* 4:4554-4563.
- Panyushkina IP, Meko DM, Macklin MG, Toonen WHJ, Mukhamedev MM, Konovalov VG, et al., 2018. Runoff variations in Lake Balkhash Basin, Central Asia, 1779-2015 inferred from tree rings. *Clim Dyn* 51:3161-77.
- Propastin P, 2012. Problems of water resources management in the drainage basin of Lake Balkhash with respect to political development, p. 449-461. In: Leal Filho W (eds.), *Climate change and the sustainable use of water resources*. Berlin: Springer.
- Pueppke SG, Iklasov MK, Beckmann V, Nurtazin ST, Thevs N, Sharakhmetov S, Hoshino B, 2018a. Challenges for sustainable use of the fish resources from Lake Balkhash, a fragile lake in an arid ecosystem. *Sustainability* 10:1234.
- Pueppke SG, Zhang QL, Nurtazin ST, 2018b. Irrigation in the Ili River Basin of Central Asia: from ditches to dams and diversion. *Water* 10:1650.
- Sala R, Deom JM, Aladin NV, Plotnikov IS, Nurtazin S, 2020. Geological history and present conditions of Lake Balkhash, p. 143-175. In: Mischke S (Ed.), *Large Asian lakes in a changing world*. Cham: Springer.
- Santos Neto EVD, Hayes JM, Takaki T, 1998. Isotopic biogeochemistry of the Neocomian lacustrine and Upper Aptian marine- evaporitic sediments of the Potiguar Basin, Northeastern Brazil. *Org Geochem* 28:361-381.
- Schwark L, Zink K, Lechterbeck J, 2002. Reconstruction of postglacial to early Holocene vegetation history in terrestrial Central Europe via cuticular lipid biomarkers and pollen records from lake sediments. *Geology* 30:463-466.
- Shen BB, Wu JL, Zhan S, Jin M, 2021a. Residues of organochlorine pesticides (OCPs) and polycyclic aromatic hydrocarbons (PAHs) in waters of the Ili-Balkhash Basin, arid Central Asia: concentrations and risk assessment. *Chemosphere* 273:129705.
- Shen BB, Wu JL, Zhan S, Jin M, Saparov A, Abuduwaili J, 2021b. Spatial variations and controls on the hydrochemistry of surface waters across the Ili-Balkhash Basin, arid Central Asia. *J Hydrol* 600:126565.
- Smol JP, 2019. Under the radar: long-term perspectives on ecological changes in lakes. *P Roy Soc B-Biol Sci* 286:1906.
- Toivonen H, Huttunen P, 1995. Aquatic macrophytes and ecological gradients in 57 small lakes in southern Finland. *Aquat Bot* 51:197-221.
- Volkman JK, Barrett SM, Blackburn SI, Mansour MP, Sikes EL, Gelin F, 1998. Microalgal biomarkers: a review of recent research developments. *Org Geochem* 29:1163-1179.
- Wan ZF, Wang XQ, Li YF, Xu X, Sun YF, Yin ZX, Guan HX, 2018. The composition and geochemical significance of organic matters in surface sediments from the Southwest Sub-basin of the South China Sea. *J Asian Earth Sci* 171:103-117.
- Wu JL, Ma L, Yu H, Zeng HA, Liu W, Abuduwaili J, 2013. Sediment geochemical records of environmental change in Lake Wuliangsu, Yellow River Basin, North China. *J Paleolimnol* 50:245-255.
- Yang B, Ljung K, Nielsen AB, Fahlgren E, Hammarlund D, 2021. Impacts of long-term land use on terrestrial organic matter input to lakes based on lignin phenols in sediment records from a Swedish forest lake. *Sci Total Environ* 774:145517.
- Zhang HL, Wu JL, Li QY, Jin M, 2021. A ~300-year record of environmental changes in Lake Issyk-Kul, Central Asia, inferred from lipid biomarkers in sediments. *Limnologia* 90:125909.